The helical-ferromagnetic phase transition in Gd-Y alloys

1992 J. Phys.: Condens. Matter 4 10045

(http://iopscience.iop.org/0953-8984/4/49/031)

J. Phys.: Condens. Matter 4 (1992) 10045–10052. Printed in the UK

The helical–ferromagnetic phase transition in Gd–Y alloys

R J Melville†, R S Eccleston†, G J McIntyre‡ and S B Palmer†
† Department of Physics, University of Warwick, Coventry, CV4 7AL, UK
‡ Institut Laue–Langevin, Grenoble, France

Received 11 September 1992

Abstract. We have carried out a neutron diffraction study on a single crystal of $Gd_{66}Y_{34}$ to examine the behaviour of the helical q-vector close to the helix–ferromagnet II transition. A novel approach to the peak fitting of the diffraction peaks has enabled inter-layer turn angles of less than 1° to be measured, establishing strong evidence to support the proposition that this is a continuous transition. We have not observed a modulated c-axis component of magnetization in the helical phase and therefore have no evidence of threefold symmetry in this system.

1. Introduction

One of the most interesting features of the Gd–Y alloy series is the existence of an apparently continuous (second-order) phase line separating two ordered magnetic phases in the temperature–concentration plane [1, 2]. This phase line (γ) exists between the compositions $Gd_{60}Y_{40}$ and $Gd_{70}Y_{30}$, separating a high-temperature simple helical phase (where the moments are confined to the hexagonal basal plane) from a low-temperature canted ferromagnetic phase, ferro II (figure 1). On approaching γ from the helimagnetic phase by lowering the temperature, the helical turn angle appears to decrease smoothly towards zero, values as small as 1.4° having been measured [1]. This suggests that a continuous change of the order parameter may take place on crossing the boundary between the helimagnetic and ferro II phases. Such behaviour, unique among rare earths, is attributable to the very low planar anisotropy of Gd and can be modelled assuming continuous basal plane anisotropy [3].

In addition to this process, as γ is crossed into the ferromagnetic phase, the magnetic moment develops a component along the hexagonal c axis. The concurrence of these two processes along the same phase line is remarkable in that there is no *a priori* reason for these processes to occur simultaneously; in simple models consistent with the hexagonal symmetry assumed for these alloys, this line would normally split into two: one associated with vanishing q, the other associated with the appearance of a c-axis moment. This seemingly accidental feature has been explained by invoking a threefold symmetry argument [4]. In this symmetry there appears a fourth order term in the Landau free energy which couples the magnetism in the basal plane $S_{\perp}$, to that along the c axis, S_c. Consequently there should exist no ferromagnetic phase for which $S_c = 0$ and this is supported by experiment. In the helical phase it is predicted that there should exist a modulated c-axis component of magnetization with wavevector $3q$, namely $S_{c,3q}$.

0953-8984/92/4910045+08$07.50

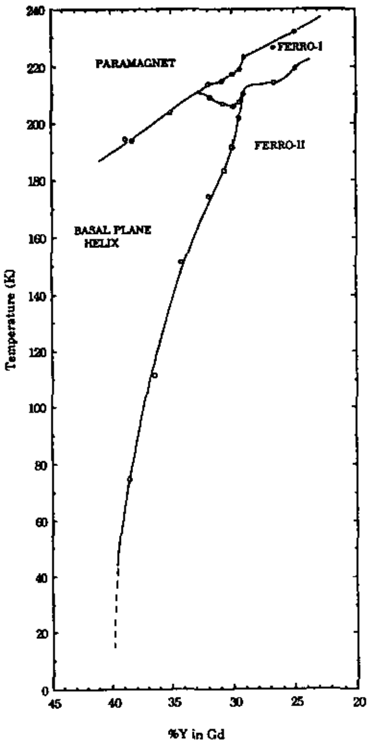

Figure 1. Magnetic phase diagram of the Gd–Y alloy series.

We have attempted to elucidate the nature of the helical–ferro II transition in Gd–Y by (1) closely examining the behaviour of the magnetic moments as this transition is crossed in $Gd_{66}Y_{34}$ and (2) looking for evidence of threefold symmetry as suggested by Barbara and Mukamel [4]. Indeed as well as explaining some of the general features of the Gd–Y system, evidence of threefold symmetry would have important implications for other rare-earth systems.

2. Experimental details

Magnetic structure determinations were carried out on $Gd_{66}Y_{34}$ using the D9 four-circle diffractometer at ILL, Grenoble, France. Due to the inherently high absorption of thermal neutrons by natural Gd, the experiment was performed at a wavelength of 0.48 Å (a compromise between high absorption at long wavelength and low flux at short wavelength). The sample was mounted with its a^*–c^* plane in the horizontal diffractometer plane to maximise the instrumental resolution along the c^* direction about $h0l$ type reflections. For the hexagonal close-packed Gd–Y structure, the ferromagnetic components of the spontaneous magnetization could be determined from the magnetic contributions to the 100 and 002 reflections and equivalents, since these in general contain contributions from both the c axis and basal components of the magnetization [5]. At each temperature, scans were also performed along various directions in reciprocal space to check for the appearance of antiferromagnetic satellite reflections. For a simple helix with the moments confined to the basal plane and q paralled to the c axis, a single pair of satellite reflections should be observed for every allowed hkl at $hk\zeta$ (where $\zeta = l \pm q$ and q is a displacement in reciprocal lattice units along c^*). The inter-layer turn angle is then given by πq. In this phase the 002 reflection also contains contributions from its associated satellites owing to the poor inherent resolution along c^* for 001 reflections.

3. Results

The average intensities I_{002} and I_{100} are plotted against temperature in figure 2. The Néel temperature for $Gd_{66}Y_{34}$ was observed to be 208 K from the appearance of antiferromagnetic satellites at $hk\zeta$. The intensity variation of satellites centred about different reciprocal lattice points indicated, together with the absence of any magnetic contribution to the 100 reflection, that the initial ordered structure is a simple basal plane helix. As the temperature was lowered through the helical phase, the q-vector of the helix was observed to decrease uniformly and approach zero at the helix–ferromagnet II transition at approximately 151 K, where the satellites became fully absorbed under the nuclear peak. At this transition to ferromagnetism, the magnetic intensity appearing on the 100 reflection indicated that the moments rapidly rotate out of the basal plane, acquiring a canting angle of about 65°. This is the canted ferromagnetic phase, ferromagnet II, which remained stable down to the lowest temperature studied (15 K).

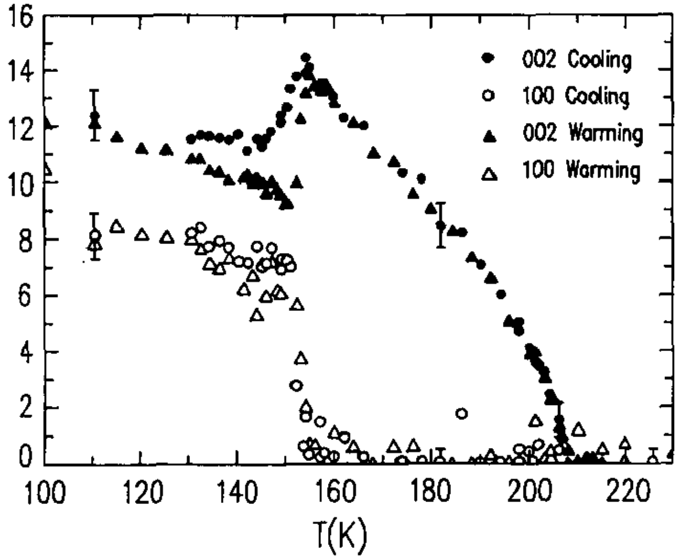

Figure 2. Temperature dependence of the integrated intensity for $Gd_{66}Y_{34}$: ●, 002 (cooling); ○, 100 (cooling); ▲, 002 (warming) and △, 100 (warming).

The behaviour of the turn angle is clearly depicted in figure 3, an isometric plot built up from c^* scans through the 101 reflection. Although it appears from figure 3 that the transition has a continuous nature, it still remains very difficult to extract small values of q due to the limitation of the instrumental resolution. Figure 4 shows a series of Q-scans along c^* through the 101 reflection as the helix–ferro II transition

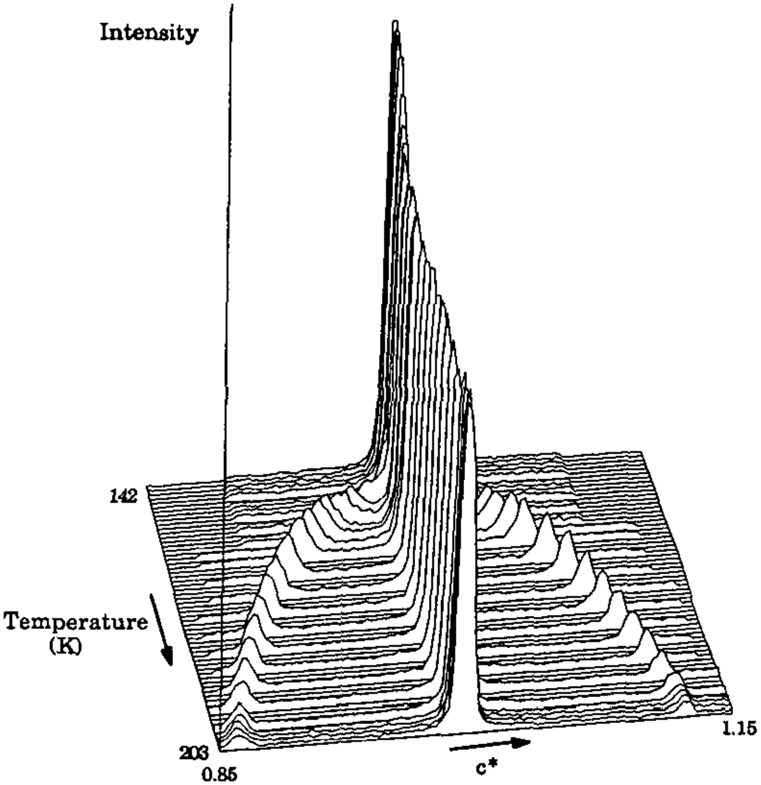

Figure 3. Isometric plot for $Gd_{66}Y_{34}$ constructed from c*-scans through the 101 reflection between 203 K and 142 K while cooling.

is approached. One can see that 3 K above the transiton the satellites begin to disappear under the strong nuclear reflection and this poses serious problems for the peak-fitting software.

We overcame this problem by constraining many of the fitting parameters so that the programme would be forced to recognise two satellites. The fitting was carried out as follows: first, the nuclear profile was fitted with two Gaussian peaks just above T_N at 208 K. This was simply an empirical device to describe the convolution of the less than perfect crystal mosaic spread with the not exactly Gaussian instrumental resolution function. The heights, widths and separation of these two peaks were then fixed, since the nuclear part of the scan was not expected to vary significantly between 208 K and 151 K, with the possible exception of the centre of this two-peak profile which was left unconstrained. The satellites, at high temperature in the helical phase, were fitted with Gaussians with the single constraint that their centres be equidistant from the centre of the main nuclear peak. This constraint alone works well until close to the ferromagnetic phase where in addition, the satellite widths were constrained to be equal and finally the heights were also constrained to be equal; a valid approximation since the satellites are so close in Q. The beauty of the method is that the magnetic intensity appearing on top of the nuclear intensity, due to the closeness of the satellites, forces the programme to fit the satellites under the main

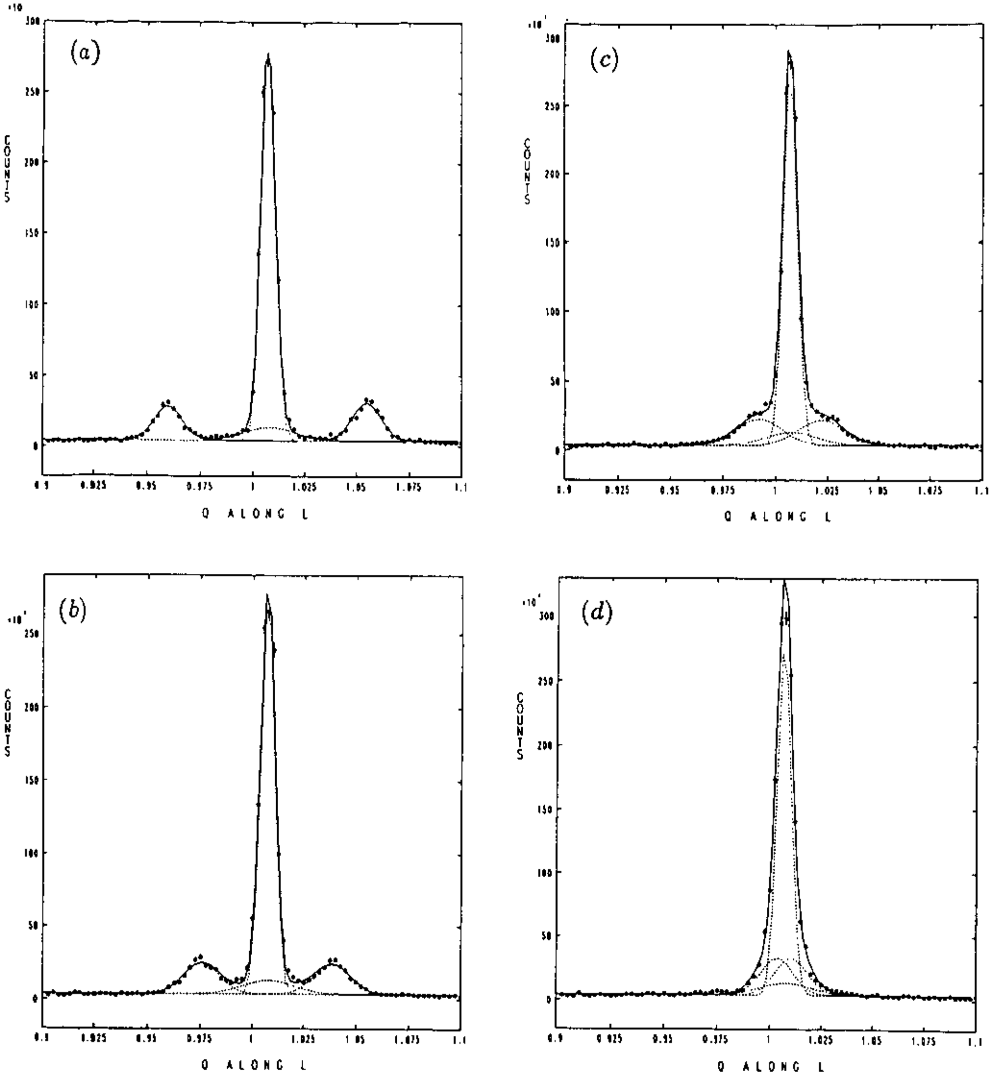

Figure 4. Q-scans for $Gd_{66}Y_{34}$ along c^* through the 101 reflection at (*a*) 157 K, (*b*) 154 K, (*c*) 152 K and (*d*) 150 K.

nuclear peak; q-vectors corresponding to a satellite separation less than the nuclear width (limited by the resolution of the instrument) have been measured by these means. The fitting from several scans near the transition is also shown in figure 4; the turn angle calculated from these fits is shown in figure 5. The overall fits are very good and this is reflected in the well behaved turn angle, which falls to values much less than 1° per layer.

It may be argued that it is meaningless to talk of a 'turn angle' when the satellites are so close together as to be indistinguishable from a single broad ferromagnetic peak. However, in an apparently continuous transition of this type, there is not so much a transition from helimagnetism to ferromagnetism, but rather the transition occurs via short-range helical order with low q and short-range ferromagnetic order.

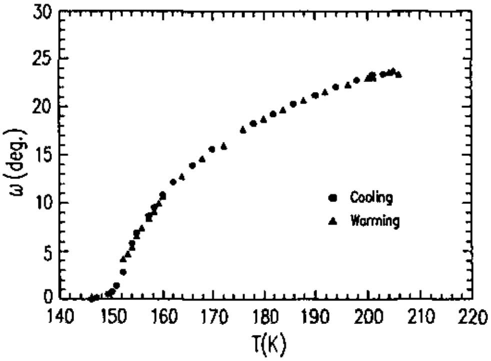

Figure 5. Temperature dependance of the helical turn angle for $Gd_{66}Y_{34}$: ●, cooling and ▲, warming.

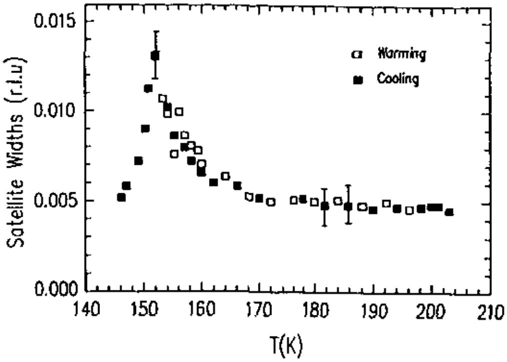

Figure 6. Temperature dependance of the satellite widths associated with the 101 reflection from $Gd_{66}Y_{34}$: □, warming and ■, cooling.

Therefore any boundary defined between the two has to be somewhat arbitrary. An indication of such a boundary might, for example, be the point at which maximum short-range order is reached. A plot of the fitted satellite widths against temperature is given in figure 6. The maximum in the widths corresponds well to T_c determined by extrapolation of the turn angle to zero. Below this temperature, the ferromagnetic regions are dominant and becoming long-range ordered. More importantly, the smooth variation of the fitted 'turn angle' to values less than 1° (indicating a good peak fit even at a temperature where short-range ferromagnetism is dominant) is strong evidence to support the proposition that the transition is continuous.

There is some small thermal hysteresis, of 2 K at most, associated with the changeover from the modulated structure to ferromagnetic structure (figure 1), as observed previously [6, 7]. Thermodynamically, this is unusual when contrasted with the smooth decrease of the q-vector to zero at the transition, which is characteristic of a second order process. However, the thermal hysteresis almost certainly arises from the nucleation of different helical domain structures between warming and cooling. This has been observed in Tb and MnP [8, 9]. From the discussion of helical and ferromagnetic domain structures by Palmer [10], there is a strong case for arguing that on cooling, the ferromagnetic domains grow directly from the low-q helical domains; on warming, however, the helical domains grow from the ferromagnetic domain walls. This would explain the sudden appearance of satellites at low but finite q in the helical phase on warming (figure 7), rather than emerging from beneath the nuclear peak in the reverse manner to the behaviour on cooling (figure 3). By using the minimum inter-layer turn angle of 4° observed on entering the helical phase from the ferromagnetic phase, and assuming this turn angle is associated with the domain walls (in the ferromagnetic phase) from which the chirality domains evolve, it is possible to estimate that there are 45 spins in a 180° Bloch wall.

We should like to conclude by making a few general comments on the paper by Barbara and Mukamel [4] which attempts to explain some features of the Gd–Y phase diagram by assuming that the system possesses threefold rather than the normally assumed sixfold symmetry. In particular, such an assumption would mean that the commensurate–incommensurate transition associated with the vanishing of the q-vector would then be accompanied by a non-zero component of the magnetization

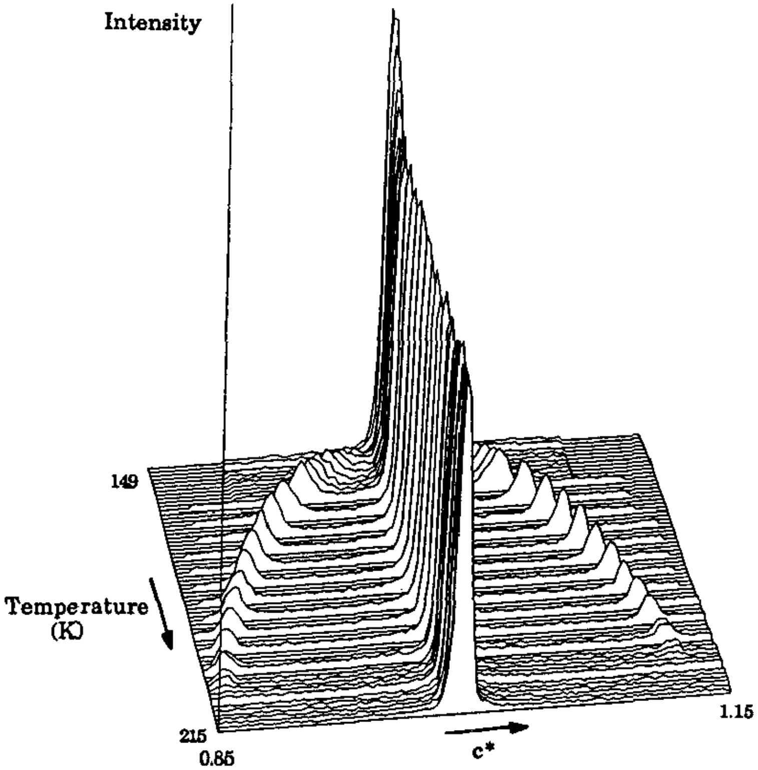

Figure 7. Isometric plot for $Gd_{66}Y_{34}$ constructed from c^* scans through the 101 reflection between 203 K and 142 K while warming.

in the ferromagnetic plane, as found experimentally. Furthermore, analysis of the Landau free energy for the threefold symmetrical system predicts that in the helical phase, the order parameter induces a modulated c-axis component $S_{c,3q}$ which is a higher harmonic of the wavevector of the basal plane magnetization $S_{\perp}$.

This prediction was tested experimentally with $Gd_{66}Y_{34}$ in the extensive helical phase. In order to check for the existence of an oscillatory c-axis component of magnetization, we carried out detailed Q-scans along c^* for reflections such as 100 and 101 and their symmetry-related counterparts, since these reflections make best use of the instrumental resolution when the crystal is mounted with the a^*–c^* plane coincident with the scattering plane. These types of scans were used, of course, to measure the satellites associated with the basal plane modulation in the helical phase. However, scans were now required across the full Brillouin half-zone, for a range of temperatures, in order to observe any c-axis modulation with $3q$ wavevector.

A typical Q-scan across a full half-zone in the helical phase of $Gd_{66}Y_{34}$ is presented in figure 8. Clearly, no $3q$ modulation is apparent and indeed none was found at any temperature in the helical phase. We therefore estimate that a modulated c-axis component of magnetization (should it exist) would have a maximum of 0.2 μB. This is rather disappointing, since it was hoped that, in addition to solving an intriguing problem in Gd–Y, evidence of threefold symmetry might have shed

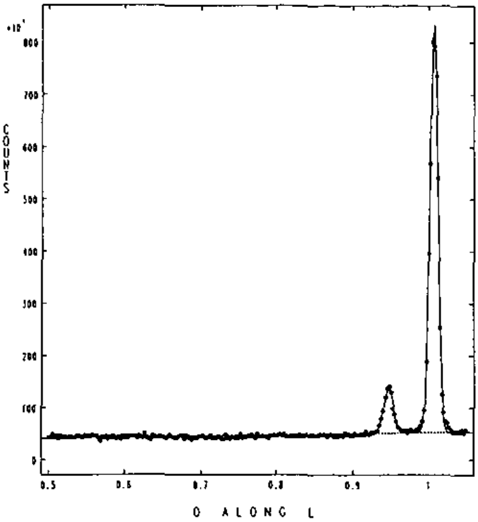

Figure 8. A Q-scan across a full half-zone (from 0.500 to 100) in the helical phase of $Gd_{66}Y_{34}$.

some light on neutron topographical studies in the rare earths. These show that the chirality domains are associated with very strong memory effects, where a particular region of the sample always retains the same sense of chirality.

Acknowledgments

The authors would like to thank M Vrtis for technical assistance and B Barbara for very helpful discussions. R J Melville and R S Eccleston acknowledge the support of the Science and Engineering Research Council.

References

[1] Bates S, Palmer S B, Sousa J B, McIntyre G J, Fort D, Legvold S, Beaudry B J and Koehler W C 1985 *Phys. Rev. Lett.* **55** 2968
[2] Palmer S B, Bates S, McIntyre G J, Sousa J B, Fort D and Beaudry B J 1986 *J. Magn. Magn. Mater.* **54–7** 519
[3] Michaleson S 1977 *Phys. Rev.* B **16** 585
[4] Barbara B and Mukamel D 1989 *J. Phys.: Condens. Matter* **1** 9057
[5] Bates S, McIntyre G J, Palmer S B and Sousa J B 1987 *J. Phys. F: Met. Phys.* **17** 1973
[6] Legvold S, Burgardt P and Beaudry B J 1980 *Phys. Rev.* B **22** 2573
[7] Blackie G N 1981 *PhD Thesis* University of Hull
[8] Baruchel J, Palmer S B and Schlenker M 1981 *J. Physique* **42** 1279
[9] Drillat A 1981 *PhD Thesis* University of Grenoble
[10] Palmer S B 1975 *J. Phys. F: Met. Phys.* **5** 2370